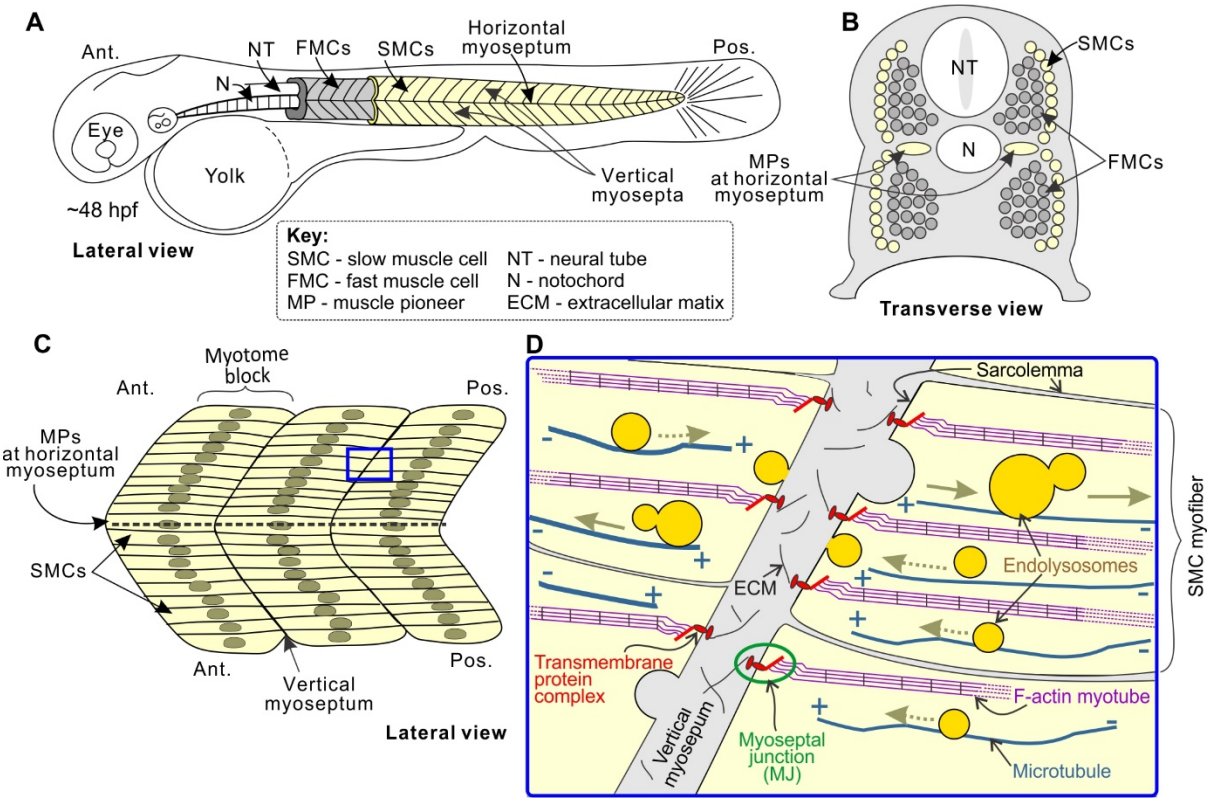

Fig. S1. Schematics to show the location of the slow muscle cells (SMCs) in the trunk of zebrafish embryos at ~24 hpf. **(A)** Lateral view of the entire embryo showing the superficial distribution of the SMCs in relation to the more deeply located fast muscle cells (FMCs). The neural tube (NT), notochord (N), and both the horizontal and vertical myosepta are also shown. **(B)** Transverse view of the trunk at ~24 hpf showing the location of the SMCs, FMCs, NT, N, and muscle pioneers (MPs) at the horizontal myoseptum. **(C)** Lateral view of the SMCs at higher magnification. The region bounded by the blue rectangle is shown in greater detail in **(D)**. **(D)** Schematic to show relevant components of the myoseptal junctions (MJs). These include the lateral end of the F-actin-rich myotubes, which are linked to extracellular matrix (ECM) components in the vertical myoseptal via the terminal sarcomeric z-lines, cortical actin cytoskeleton, and transmembrane protein complexes. Microtubules (with their plus and minus ends) and endolysosomes are also shown. Ant. and Pos. are anterior and posterior, respectively. Not drawn to scale.

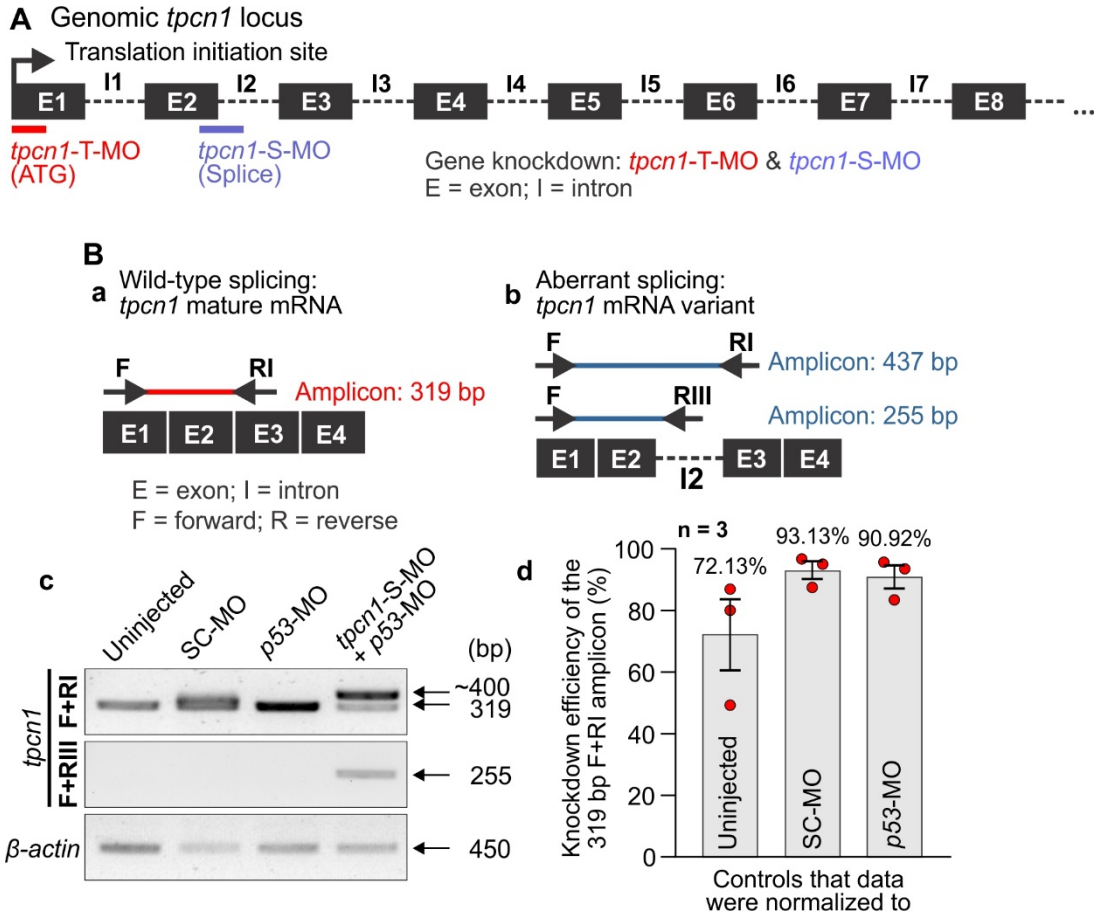

Fig. S2. Design and evaluation of two independent MOs that target the *tpcn1* transcripts in zebrafish. (A) A translation-blocking *tpcn1*-MO (*tpcn1*-T-MO) was designed to bind to a region spanning the start codon of the principal *tpcn1* splice variant in zebrafish (*tpcn1-202*; Ensembl transcript ID: ENSDART00000138123.4), and the splice-blocking *tpcn1*-MO (*tpcn1*-S-MO) bound to an exon-intron junction common to all three *tpcn1* transcripts (*tpcn1-201*: ENSDART00000090102.6; *tpcn1-202*; *tpcn1-203:* ENSDART00000187745.1). **(Ba)** Schematic of the wild-type *tpcn1* mRNA transcript (with exons 1-4 alone) showing the design of one forward (F) and one reverse (RI) primer for performing reverse-transcription PCR (RT-PCR). **(Bb)** A possible aberrant *tpcn1* mRNA transcript containing intron 2, which might result from the splice-blocking action of the *tpcn1*-S-MO (again only exons 1-4 are shown). The design of another reverse primer (RIII) to detect intron-inclusion is also shown. **(Bc,Bd)** RT-PCR analyses of *tpcn1* transcripts following *tpcn1*-S-MO-mediated knockdown resulted in aberrant mRNA splicing, which was characterized as intron inclusion. **(Bc)** A representative 2% agarose gel showing the RT-PCR products after the F+RI and F+RIII primer sets were used to amplify different portions of the *tpcn1* mRNA transcript. *β-actin* was used as the internal control. **(Bd)** Bar chart to show the mean ± SEM knockdown efficiency of the *tpcn1*-S-MO, which was evaluated from agarose gels, such as the one shown in **(Bc)**. When normalized to the *p53*-MO controls, the knockdown efficiency of normal *tpcn1* transcripts in *tpcn1*-S-MO- + *p53*-MO-injected embryos was ~90.9%.

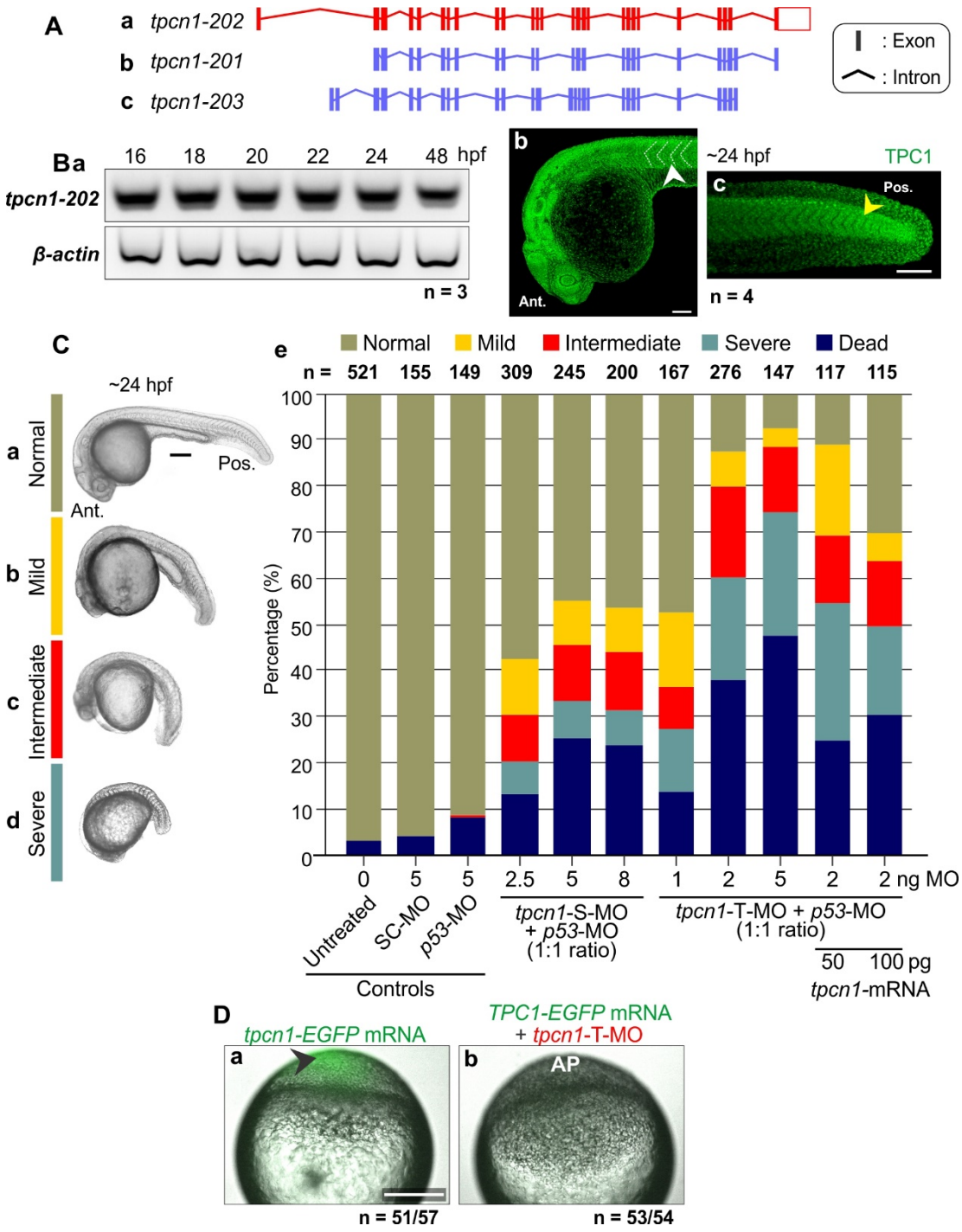

Fig. S3. The *tpcn1* variants in zebrafish, expression of *tpcn1-202* mRNA and TPC1 protein in embryos, dose-dependent effect of the *tpcn1*-MOs (with/without mRNA rescue) on zebrafish development at ~24 hpf and effect of the *tpcn1*-T-MO on the expression of TPC1-EGFP. (A) Schematics of the three transcript variants of *tpcn1* in zebrafish, with the principal isoform (*tpcn1-202*) shown in red. **(Ba)** Representative cDNA gel to show the expression of *tpcn1-202* mRNA in embryos from 16 hpf to 48 hpf. At each time point, RNA was extracted from excised trunks and subjected to RT-PCR. The *β-actin* house-keeping gene was used as a loading control. These data show

that the *tpcn1-202* transcript is expressed in embryos at ~16 hpf (during the segmentation period) when the somites are forming. However, evidence on a publicly available transcriptomic database (Expression Atlas; https://www.ebi.ac.uk/gxa/home) indicates that *tpcn1* (ensdarg00000062362) is expressed as early as the zygote and cleavage stages in zebrafish. **(Bb,Bc)** Expression of TPC1 at ~24 hpf (i.e., ~30 somite stage) in **(Bb)** mature anterior somites (white arrowhead), and **(Bc)** immature forming somites in the tail (yellow arrowhead). **(C)** Injection of the different *tpcn1*-MOs (or the *tpcn1*-T-MO plus *tpcn1-202* mRNA) at the 1-cell stage generated a range of different phenotypes by ~24 hpf. Representative examples of these phenotypes are shown in the bright-field images **(Ca-Cd)**. Embryos were defined as: **(Ca)** being grossly normal; having **(Cb)** mild, **(Cc)** intermediate or **(Cd)** severe deformities; or dead. **(Ce)** Stacked bar graph showing the percentage of embryos that exhibited a particular phenotype at ~24 hpf. The embryos were either untreated or else they were injected at the 1-cell stage with: 5 ng standard control- (SC-) MO; 5 ng *p53*-MO; *tpcn1*-S-MO + *p53*-MO at a 1:1 ratio from 2.5 ng – 8 ng; *tpcn1*-T-MO + *p53*-MO at a 1:1 ratio from 1 ng -5 ng; or 2 ng *tpcn1*-T-MO + 2 ng *p53*-MO plus 50 pg or 100 pg *tpcn1-202* mRNA. Both the *tpcn1*-T-MO and *tpcn1*-S-MO produced a dose-dependent response with regards to the numbers of embryos exhibiting differing amounts of phenotypic disruption or death. When one-cell stage embryos were injected into the yolk with the *tpcn1*-T-MO and into the blastodisc with a *tpcn1* 'rescue' mRNA construct, there was a partial rescue of the MO-induced phenotype. In **(B)** and **(C)**, ant. and pos, are anterior and posterior, respectively. **(D)** Representative examples of embryos injected with *in vitro* synthesized mRNA encoding enhanced green fluorescent protein (EGFP) tagged to the C-terminus of TPC1 (*tpcn1-EGFP* mRNA) either **(Da)** alone or **(Db)** with the *tpcn1*-T-MO. These are EGFP (green) fluorescence images superimposed on the corresponding bright-field images of shield stage (~6 hpf) embryos. In the presence of *tpcn1*-T-MO, the number of embryos with observable fluorescence (i.e., to ~1.85%), when compared with embryos injected with *tpcn1-EGFP* alone (i.e., ~89.5%). EGFP fluorescence is indicated by black arrowhead and AP is animal pole. The images are representative of 3 biological replicates each containing ~15 embryos per treatment condition. Scale bars, 100 µm **(Bb,Bc)** and 200 µm **(C,D)**.

B

Gene	Exon	Target sequence + PAM (5' to 3')	Genomic location	Exon strand	G/C content (%)	Position from 5' end of CDS
tpcn1	5	GGCTCTTGT GACGCGCAG GTGGG	chr5:23215209 -23215228	-	65	562
tpcn1	8	GGCGTATTC GAAGAATCG TTGG	chr5:23216918 -23216936	+	47	836

C

Exon	n-number	% of mutant allele in F_1 progeny of founder
5	16	68.75

D

Zebrafish line (stable CRISPR/ Cas9 F_1 adults)	Genomic sequence	Net change in sequence length	Predicted protein change
WT Exon 5	CGTCCCACCTGCGCGTCACAAGAGCC CTGC	-	-
Exon 5	CGTCCCACCaaagcaaagactcttg TGCGCGTCACAAGAGCCCTGC	+16 (16 in)	*p.(Leu189 Glnfs*42)*

E

tpcn1-/- mutant F_2 Mendelian proportion	Homozygous WT (+/+)	Heterozygous mutant (+/-)	Homozygous mutant (-/-)
Expected frequency (%)	**25.0**	**50.0**	**25.0**
Exon 5 frequency (%)	22.7	63.6	13.6

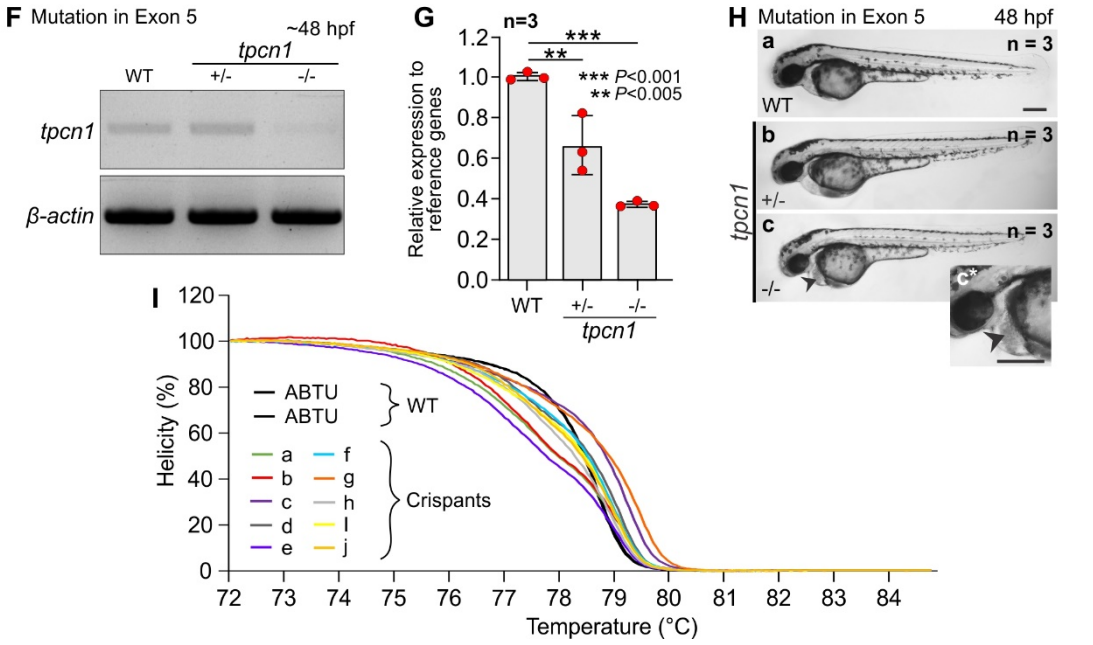

Fig. S4. Design and evaluation of gene knockdown by CRISPR/Cas9. Two single guide RNAs (sgRNAs) were selected that had the lowest number of predicted off-target sites that would target regions common to all three *tpcn1* transcript variants in zebrafish. **(A)** The genomic locus of zebrafish *tpcn1*, showing exons (E) 1-8, introns (I) 1-7, and the location of the E5 and E8 sgRNAs. **(B)** Table to show the *tpcn1* sgRNA target (PAM) sequence (in red) and information about the genomic location, exon number, strand orientation, G/C content and position from the 5' end of the coding region. **(C,D)** Of the embryos injected with exon 5 sgRNA + *Cas9* mRNA and raised to adulthood, several stable F_1 heterozygotes with indels in *tpcn1* were identified from which a single line containing a 16-base pair (bp) insertion was bred to homozygosity. **(C)** Table showing the percentage of mutant alleles identified in the F_1 progeny after outcrossing the F_0 *tpcn1* mosaic line to ABTU wild-type fish. **(D)** Indel mutation

identified within the CRISPR/Cas9 target site in a stable F_1 clutch generated by outcrossing F_0 *tpcn1* mosaic fish to the ABTU wild-type line. In the wild-type sequence of exon 5, the target site is underlined. In the mutant sequence, insertions (in) are represented by lower case red letters. The net change in length is given and the predicted protein change is described using standard nomenclature. **(E)** Frequency of homozygous wild-type (WT; +/+), heterozygous *tpcn1* mutant (+/-) and homozygous *tpcn1* mutant (-/-) zebrafish from a *tpcn1*+/- incross (n=32 fish from 3 clutches). **(F,G)** This line possessed a frameshift mutation, which was predicted to express a truncated form of the TPC1 protein less than half the length of the wild-type protein (i.e., 231 amino acids (aa) out of 805 aa in the principal TPC1 protein isoform). It was therefore expected to be missing the highly conserved activation and ion-conducting regions crucial to TPC1 function. RT-PCR and qRT-PCR of *tpcn1* mRNA in *tpcn1* homozygotes revealed a significant reduction relative to wild-type, suggesting nonsense-mediated decay (Conti and Izaurralde, 2005) **(F)** RT-PCR gel comparing the level of *tpcn1* transcript between the ABTU wild-type, *tpcn1-/+* and *tpcn1-/-* embryos. *β-actin* was used as the loading control. **(G)** mRNA expression levels of *tpcn1* determined by qRT-PCR (relative to *actb2, mob4, lsm12b* and *elfa*) in ~48-hpf ABTU wild-type, *tpcn1+/-* and *tpcn1-/-* embryos (n=3 clutches; performed in triplicate). The data are presented as mean ± SEM (as well as individual data points), and were compared using one-way ANOVA and Tukey's multiple-comparison test. **(H)** Representative bright-field extended depth-of-field images showing examples of ABTU wild-type, *tpcn1-/+* and *tpcn1-/-* embryos at ~48 hpf. The black arrowheads in **(Hc)** and **(Hc*)** indicate the accumulation of blood cells in the heart of the *tpcn1* mutants. Otherwise, the mutants were mostly comparable to ABTU wild-type embryos at ~48 hpf. We found that ~40% of the heterozygous embryos could be grown to adulthood for breeding purposes. Scale bar, 1 mm. **(I)** To generate *tpcn1* crispants, wild-type embryos were injected with the *tpcn1* exon 8 sgRNA + *Cas9* mRNA. These embryos were individually genotyped using high resolution melt analysis (HRMA) after phenotypic analysis was performed on immunolabelled embryos. The shift in melting curves amplified from individually genotyped ~48 hpf *tpcn1* crispant embryos compared to wild-type embryos, was used as an indicator that the *tpcn1* exon 8 sgRNA was effective in generating Cas9-mediated indels at its *tpcn1* target sequence. This HRMA line graph shows the *tpcn1* crispants (n = 10) and ABTU-wildtypes (n = 2).

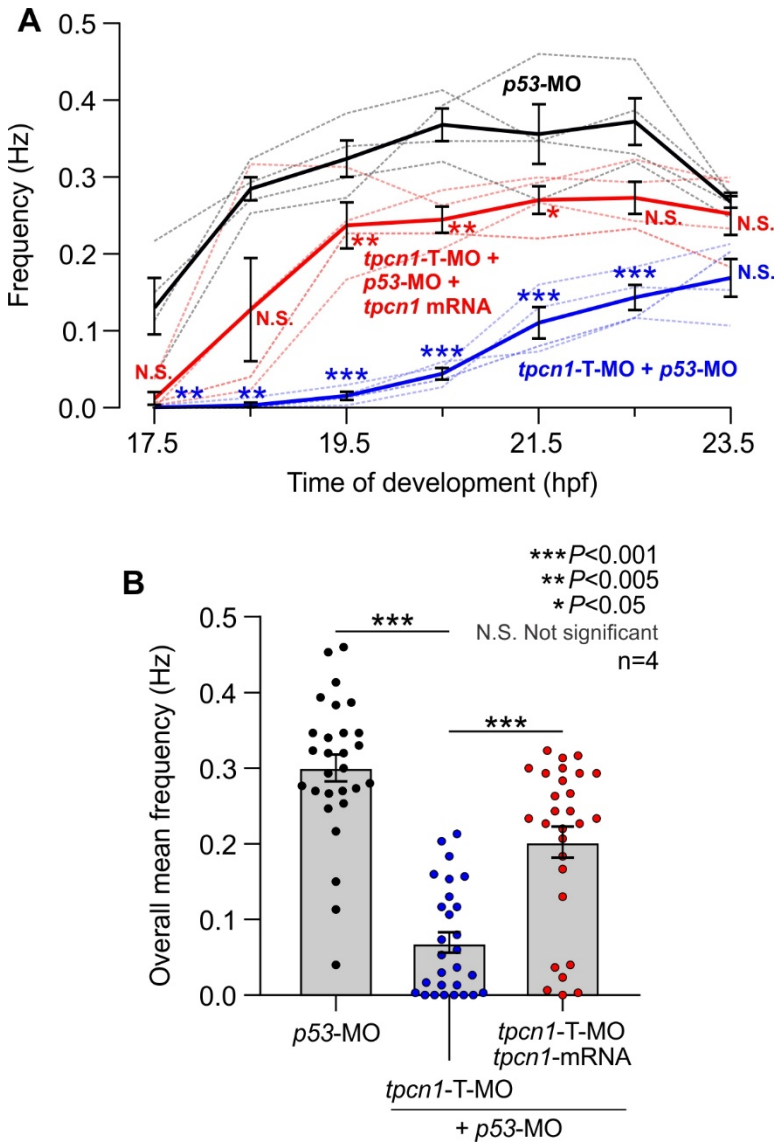

Fig. S5. Effect of MO-based knockdown on the spontaneous coiling behaviour of embryos from ~17.5 hpf to ~23.5 hpf. **(A)** Line graph to show the spontaneous coiling frequency (calculated at 1-h intervals between ~17.5 hpf and ~23.5 hpf) of embryos that were injected with: *p53*-MO; *tpcn1*-T-MO + *p53*-MO; or *tpcn1*-MO + *p53*-MO + *tpcn1* mRNA (n=4 for each). The mean ± SEM spontaneous coiling frequency (solid lines) and the data from individual experiments (dashed lines) observed during the first 5 min at each time point. **(B)** Bar graph (with individual value points) to show the overall mean ± SEM spontaneous coiling frequency from ~17.5 hpf to ~23.5 hpf across the different treatment groups. In both graphs the *tpcn1*-T-MO + *p53*-MO data were compared statistically with the *p53*-MO data, whereas the *tpcn1*-MO + *p53*-MO + *tpcn1* mRNA data were compared with the *tpcn1*-T-MO + *p53*-MO data. Spontaneous coiling behaviour was chosen for comparison because it results mainly from excitation-contraction of SMCs (Naganawa and Hirata, 2011; Hirata et al., 2012).

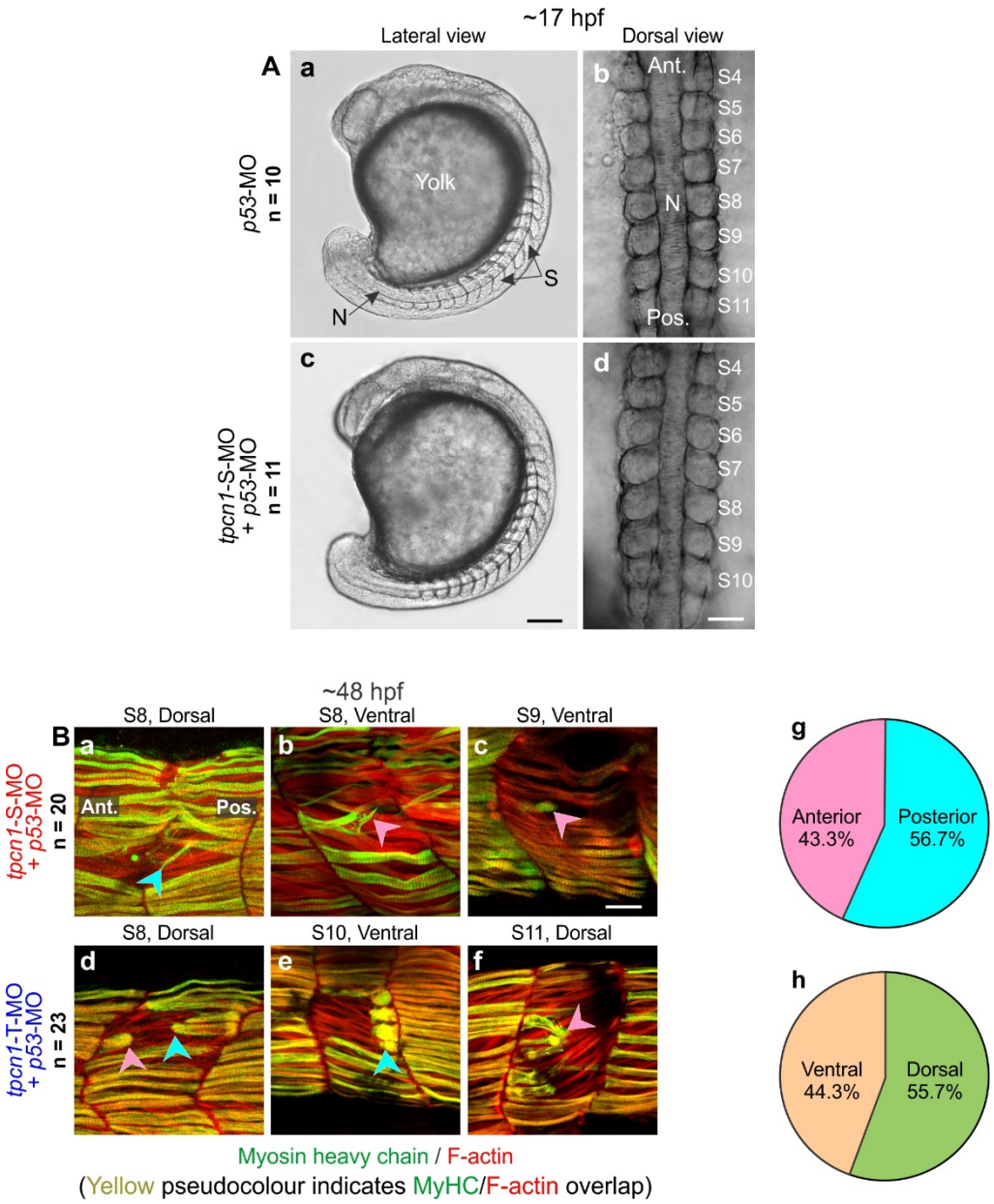

Fig. S6. Effect of MO-based knockdown of TPC1 on somite formation at ~17 hpf and the location of SMC detachments at ~48 hpf. (A) Embryos were injected at the 1-cell stage with **(Aa,Ab)** *p53*-MO or **(Ac,Ad)** *tpcn1*-S-*MO + p53*-MO, and bright-field images were acquired from the **(Aa,Ac)** lateral and **(Ab,Ad)** dorsal views at ~17 hpf. **(B)** Embryos were injected at the 1-cell stage with **(Ba-Bc)** *tpcn1*-S-*MO + p53*-MO or **(Bd-Bf)** *tpcn1*-T-MO + *p53*-MO. They were fixed at ~48 hpf and then immunolabeled with an antibody to myosin heavy chain (green) and co-labelled with fluorescent phalloidin to reveal the localisation of F-actin (red). S8-S11 indicate somites 8-11, respectively. The pink and blue arrowheads indicate SMCs detached on the anterior and posterior ends of the myotome boundaries, respectively. **(Bg,Bh)** Pie charts to show the proportion of detachments that occurred from the **(Bg)** anterior or posterior, and **(Bh)** ventral or dorsal regions of somites. Ant. and Pos. are anterior and posterior, respectively. Scale bars, 200 µm **(Ac)**, 50 µm **(Ad)**, and 20 µm **(B)**.

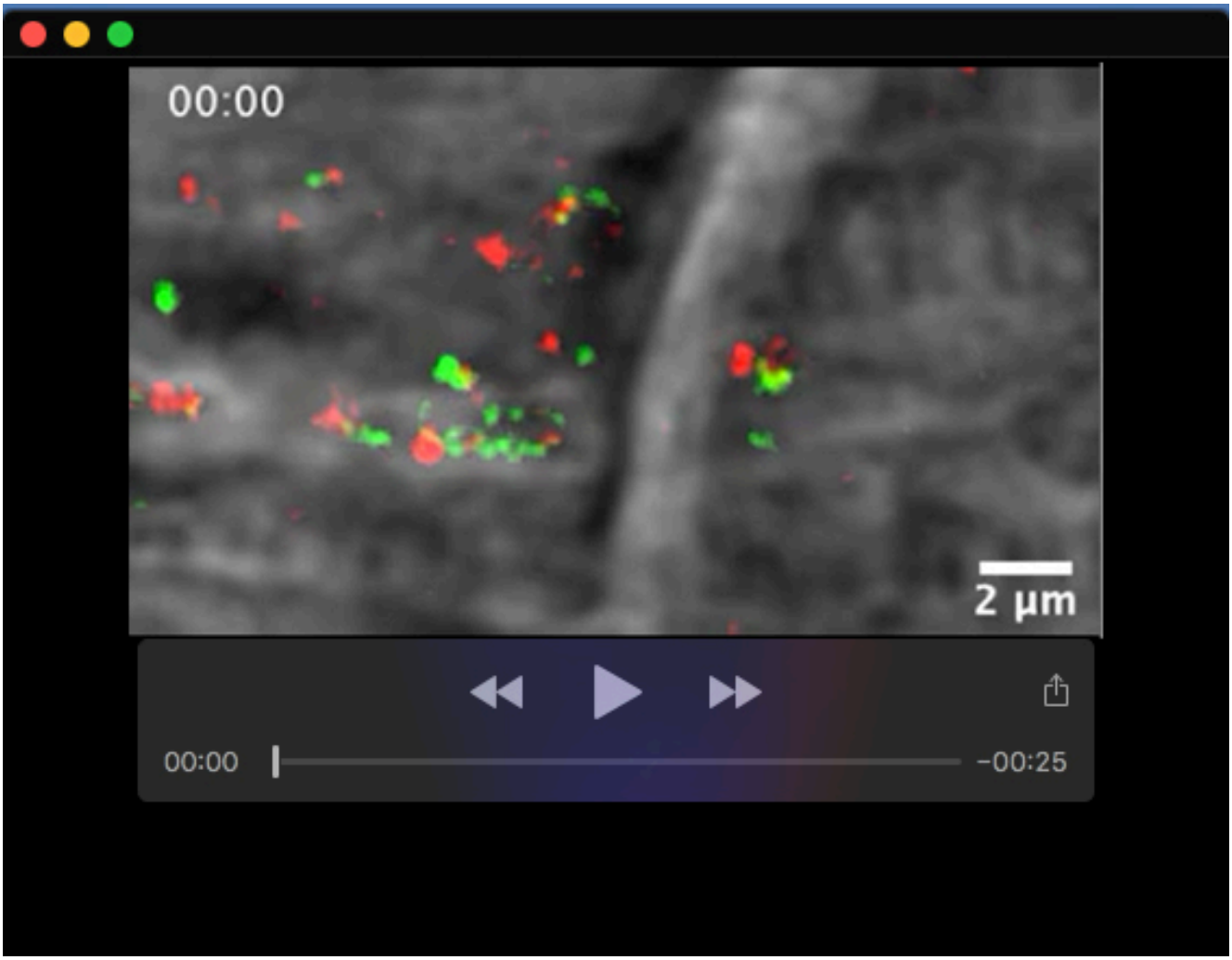

Movie 1. Time-series showing TPC1-decorated vesicles moving in an anterograde direction towards the MJ (pink arrow), and in a retrograde direction from the MJ (blue arrow) in the SMCs of an intact ~24 hpf embryo.

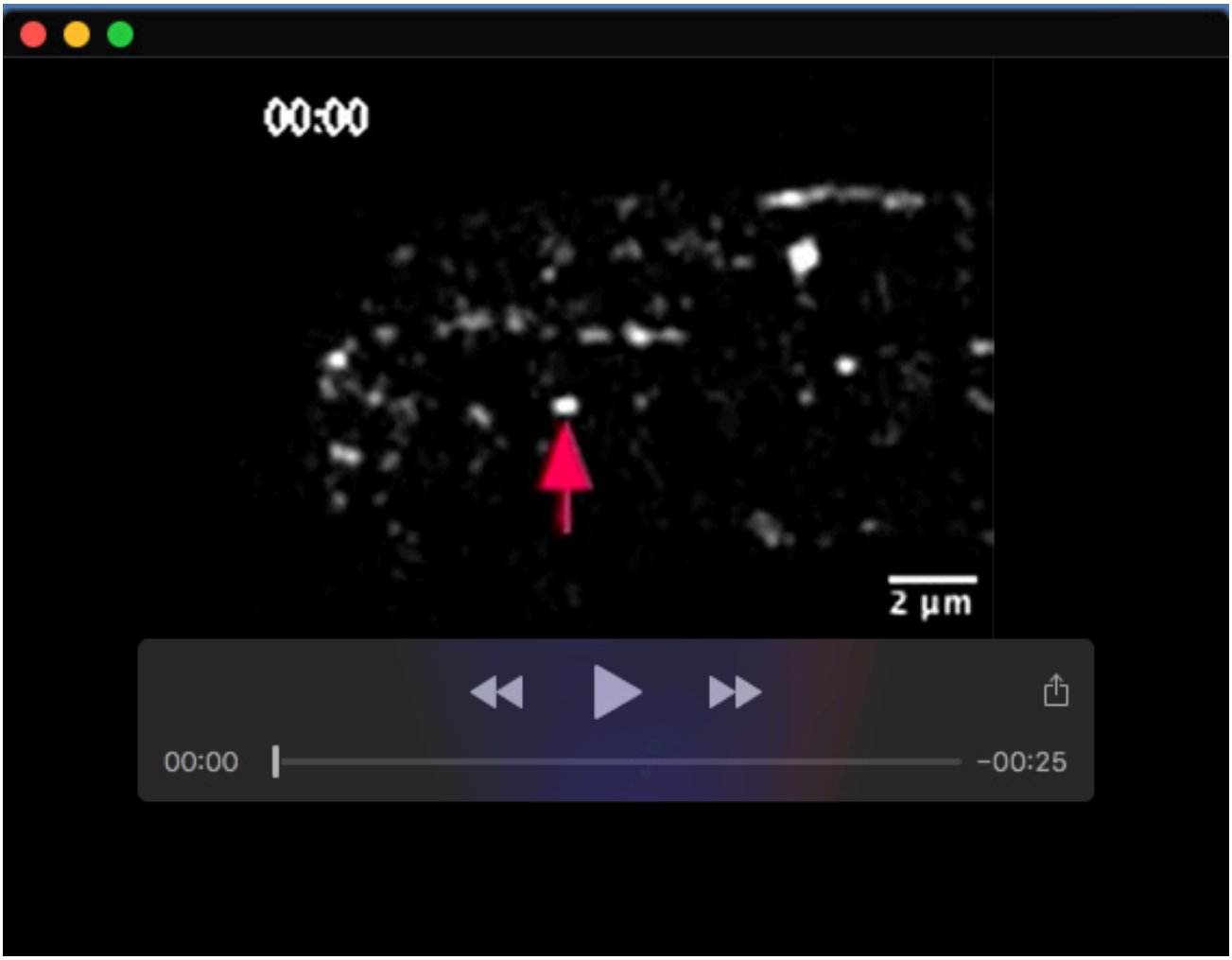

Movie 2. Time-series showing a TPC1-decorated vesicle (see pink arrow) moving in an anterograde direction towards the MJ at the end of a primary cultured SMC.

References

Conti, E. and Izaurralde, E. (2005). Nonsense-mediated mRNA decay: Molecular insights and mechanistic variations across species. *Curr. Op. Cell Biol*. **17**, 316-325. doi:S0955-0674(05)00047-5

Hirata, H., Wen, H., Kawakami, Y., Naganawa, Y., Ogino, K., Yamada, K., Saint-Amant, L., Low, S.E., Cui, W.W., Zhou, W., Sprague, S.M., Asakawa, K., Muto, A., Kawakami, K. and Kuwada, J.Y. (2012). Connexin 39.9 protein is necessary for coordinated activation of slow-twitch muscle and normal behaviour in zebrafish. *J. Biol. Chem.* **287**, 19080-1089. doi:10.1074/jbc.M111.308205.

Naganawa, Y. and Hirata, H. (2011). Developmental transition of touch response from slow muscle-mediated coilings to fast muscle-mediated burst swimming in zebrafish. *Dev. Biol.* **355**, 194-204. doi: 10.1016/j.ydbio.2011.04.027